Research and Development Journal
Volume 26 Issue 2 April-June 2015

Received 1 August 2014 Accepted 23 March 2015

DETERMINATION OF SAFE WITHDRAWAL RATES OF COMPRESSED-AIR ENERGY STORAGE IN SALT CAVERNS

The Engineering Institute of Thailand under H.M. The King's Patronage

The Engineering Institute of Thailand under H.M. The King's Patronage

DETERMINATION OF SAFE WITHDRAWAL RATES OF COMPRESSED-AIR ENERGY STORAGE IN SALT CAVERNS

Suratwadee Sartkaew[1] and Kittitep Fuenkajorn[2]

[1]Student, Geomechanics Research Unit, Suranaree University of Technology, Thailand

[2]Professor, Geomechanics Research Unit, Suranaree University of Technology, Thailand

ABSTRACT

The objective of this study is to determine effects of loading rate on compressive strength and deformability of the Maha Sarakham salt under elevated temperatures. The effort is aimed at determining the safe maximum withdrawal rates for the compressed-air energy storage (CAES) in salt caverns. The constant axial stress rates range from 0.0001 to 0.1 MPa/s. The testing temperatures are maintained constant between 273 and 373 Kelvin. To incorporate the thermal and rate (time-dependent) effects into a strength criterion the distortional strain energy at dilation of the salt is calculated as a function of the mean strain energy density. Finite difference analyses (FLAC 4.0) are performed to determine the stresses and strains at the boundaries of CAES caverns for various reduction rates of the internal pressures. The maximum stresses and strains obtained during retrieval period are used to calculate the strain energy density induced at the cavern boundaries. The results are compared against the criterion developed above, and hence the safe maximum withdrawal rate of the compressed-air can be determined.

KEYWORDS: Creep, Thermal Effect, Strain Energy, Compression Test

1. Introduction

The loading rates and temperatures affect the mechanical behavior of salt around compressed-air energy storage (CAES) caverns during withdrawal period. The compressive strength and deformability of rock salt are therefore an important consideration for the design and analysis of the storage caverns when the internal pressures are continuously fluctuated. The mechanical behavior of rock salt for underground storage has been studied for many decades [1-6]. It has been found that the salt strength increases with increasing strain and loading rates. The influence of temperature variation on the strength and deformation behavior in rock salt has been widely recognized [7-8]. It is agreed that the rock strength and elastic properties decrease as temperature increases. Study on the effect of temperature and loading rate on the salt compressive strength and creep deformation has however never been attempted.

The objective of this study is to experimentally assess the influence of loading rate on compressive strength and deformability of the Maha Sarakham salt under elevated temperatures. Uniaxial compression tests have been performed using a compression load frame with applied loading rates of 0.0001, 0.001, 0.01 and 0.1 MPa/s, and temperatures of 273, 303, 343 and 373 Kelvin. The results are applied to demonstrate the impacts of loading rate and temperature on determination of the safe maximum withdrawal rate in CAES cavern.

2. Sample Preparation

The salt specimens are prepared from salt cores drilled from depths ranging between 270 and 330 m by Siam Submanee Co., Ltd. in the northeast of Thailand. The salt cores belong to the Lower Salt member of the Maha Sarakham formation. The origin and geologic sequence of the Maha Sarakham salt are described by Tabakh et al. [9]. The cores are dry-cut to obtain cylindrical shaped specimens with nominal dimensions of 47 mm diameter and 118 mm length. The average density is measured as 2.20 ± 0.02 g/cm^3. No bedding is observed in the specimens. To test the salt specimens under elevated temperatures, they are wrapped with heating tape, foil and insulator for 24 hours before testing. The low temperature specimens are placed in cooling chamber for 24 hours before testing. As a result the specimen temperatures are assumed to be uniform and constant with time during the mechanical testing (i.e., isothermal condition).

3. Test Method

The uniaxial compression tests have been performed to determine the time-dependent properties of the Maha Sarakham salt. After installing the salt specimen into compression load frame, it is axially loaded using a hydraulic cylinder and electronic pump. An electronic load cell is used to measure the load increment. The specimen deformations are monitored and used to calculate the principal strains during loading. For the low temperature testing (273 Kelvin) the salt specimen and load frame are placed in a cooling chamber for 24 hours before the loading is started. A thermocouple connected to a data recorder monitors the specimen temperature. The cooling chamber allows taking the load and strain measurements during testing. It can maintain temperature to the nearest ±2 Kelvin. For the high temperature testing (343 to 373 Kelvin) heating tapes connected to a temperature regulator, thermostat and power supply are wrapped around the specimen to maintain the desired temperatures while loading. The specimen is heated for 24 hours before loading is started. The temperatures can be maintained to the nearest ±5 Kelvin.

4. Test Results

Table 1 summarizes the results from all salt specimens. Under the same loading rate ($\partial\sigma_1/\partial t$), the compressive strength (σ_c) decreases with increasing specimen temperatures. The mean stresses (∂_m) and strains (ε_m) and octahedral shear stresses ($\tau_{Oct,f}$) and shear strains ($\gamma_{oct,f}$) at failure are determined using the relations given by Jaeger et al. [10]. The applied octahedral shear stresses are plotted as a function of octahedral shear strain in Figure 1. The measured stress-strain relations tend to be nonlinear, particularly under high temperatures. Higher loading rates applied result in higher shear strengths and lower shear strains at failure. The effect of the loading rate on the salt strength becomes larger under higher temperatures.

5. Creep Strains

To analyze the time-dependent behavior of the salt specimens, the total strain (ε_c) is divided here into two parts; elastic strain, ε^e_c, (linear and recoverable strain) and plastic creep strain, ε^c_c, (time-dependent and nonrecoverable strain). The exponential creep law [3] is used to describe the time-dependent strain of the salt. The octahedral shear stress can be derived in the forms of the octahedral shear strain:

$$\tau_{oct} = \alpha \cdot \tau_{oct}^{\beta} \cdot t^{\kappa} \cdot \exp(-\lambda / T) \tag{1}$$

where α, β, κ and λ are empirical constants, t is elapsed time and T is the constant temperature in Kelvin. For the stress rate controlled condition the octahedral shear strain at any loading time can be represented by:

$$\gamma_{oct} = \frac{\dot{\tau}_{oct} \cdot t}{2(-\psi \cdot T + G_0)} + \alpha \cdot \tau_{oct}^{\beta} \cdot t^{\beta+\kappa} \cdot \exp(-\lambda / T) \tag{2}$$

Table 1 Salt strengths and elastic properties under various loading rates and temperatures

Temperature (Kelvin)	$\partial\sigma_1/\partial\tau$ (MPa/s)	σ_1 (MPa)	σ_m (MPa)	ε_m (10^{-3})	$\tau_{oct,f}$ (MPa)	$\gamma_{oct,f}$ (10^{-3})	E (GPa)	ν
273	0.1	38.8	12.9	14.6	18.3	53.0	29.6	0.33
	0.01	34.9	11.7	17.0	16.5	54.6	28.4	0.34
	0.001	33.2	11.1	17.6	15.7	56.4	26.5	0.31
	0.0001	29.8	9.9	19.9	14.0	57.0	25.8	0.32
303	0.1	37.2	12.8	20.8	17.6	64.2	25.3	0.31
	0.01	34.6	11.5	22.7	16.3	65.2	24.2	0.35
	0.001	32.6	10.9	24.5	15.4	69.7	23.6	0.34
	0.0001	29.2	9.7	25.3	13.8	72.6	21.1	0.34
343	0.1	35.8	12.6	21.4	16.9	81.4	19.7	0.34
	0.01	33.5	11.2	24.6	15.8	83.8	18.4	0.37
	0.001	31.1	10.4	26.1	14.7	93.0	16.9	0.34
	0.0001	26.6	8.9	27.5	12.5	96.9	15.3	0.42
373	0.1	34.6	11.5	29.7	16.3	100.9	14.5	0.35
	0.01	31.5	10.5	31.4	14.9	112.5	13.1	0.32
	0.001	28.1	9.4	36.0	13.3	117.6	12.4	0.32
	0.0001	25.2	8.4	48.2	11.9	125.7	11.0	0.38

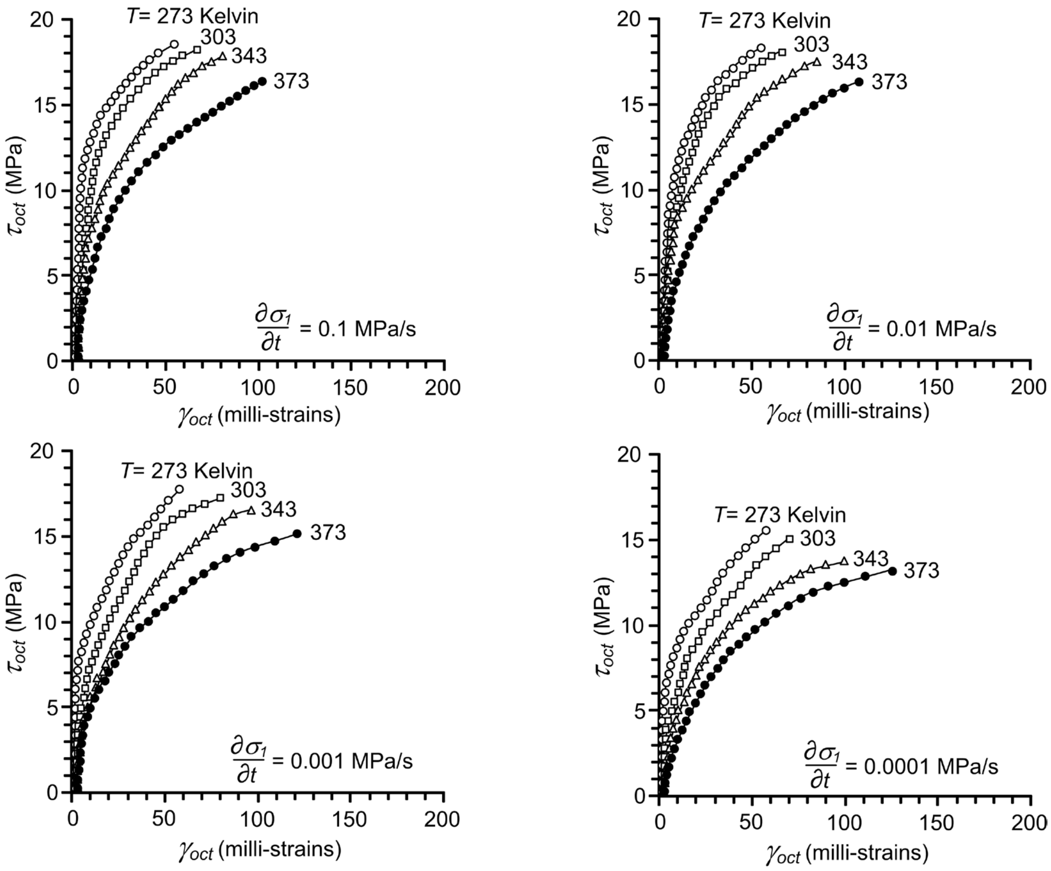

Figure 1 Octahedral shear stresses (τ_{oct}) as a function of octahedral shear strain (γ_{oct}) for various loading rates ($\partial\sigma_1/\partial t$) and temperatures ($T$)

where γ_{oct} is the octahedral shear strain, $\dot{\tau}_{oct}$ is the octahedral shear stress rate (in MPa/s), t is time (in seconds), G_0 is shear modulus at 0 Kelvin and ψ is an empirical constant. For the Maha Sarakham salt they are defined as ψ = -54.044 GPa×Kelvin^{-1}; G_0 = 25.822 GPa; α = 0.01 GPa^{-1}; β = 2.018; κ = 0.129; λ = 1559.242 Kelvin. Good correlation (R^2 = 0.954) between the proposed equation and the test results is obtained. This equation can be used to predict the time-dependent deformation of salt under various constants temperatures.

6. Octahedral Shear Strength and Shear Rate Relation

The octahedral shear stresses and strains at failure and at dilation can be calculated from the principal stresses and the principal strains. Here the dilation is defined as the stress where the volumetric strain is deviated from compression to tension. Empirical equations are proposed to predict the octahedral shear strength and dilation under various octahedral shear stress rates and temperatures as follows:

$$\tau_{oct,f} = \ln(\partial\tau_{oct}/\partial t)\cdot э + \exp(\eta/T) + \iota \qquad \text{(MPa)} \qquad (3)$$

$$\tau_{oct,d} = \ln(\partial\tau_{oct}/\partial t)\cdot э' + \exp(\eta/T) + \iota' \qquad \text{(MPa)} \qquad (4)$$

where $\ni$, $\ni'$, η, η', ι and ι' are empirical constants for the salt at failure and at dilation. The unit of shear rate ($\partial\tau_{oct}/\partial t$) and temperature ($T$) are MPa/s and Kelvin. The empirical constants are defined by regression analysis as: $\ni$ = 0.613 s^{-1}; $\ni'$ = 0.393s^{-1}; η = 460.323 MPa·Kelvin ; η' = 421.015 MPa·Kelvin; ι = 14.936 MPa and ι' = 5.766 MPa. Good correlation is obtained (R^2 = 0.962 at failure and R^2 = 0.874 at dilation).

7. Octahedral Shear Strength and Shear Strain Relation

This section proposes the shear strength and dilation criteria that take the corresponding shear strains into consideration. From the test results the octahedral shear strength can be calculated as a function of shear strain at failure and at dilation for various shear rates and temperatures. The empirical equations can be written as:

$$\tau_{oct,f} = \varpi \cdot \gamma_{oct,f}^{\vartheta} + \ln(\partial\tau_{oct}/\partial t)\cdot\varsigma + \exp(\varphi/T) \quad \text{(MPa)} \tag{5}$$

$$\tau_{oct,f} = \varpi \cdot \gamma_{oct,f}^{\vartheta'} + \ln(\partial\tau_{oct}/\partial t)\cdot\varsigma' + \exp(\varphi'/T) \quad \text{(MPa)} \tag{6}$$

where ϖ, $\varpi'\times$, ϑ, ϑ', ς, ς', φ and $\varphi'$are empirical constants for the salt at failure and at dilation. The unit of shear strain (γ_{oct}), shear rate ($\partial\tau_{oct}/\partial t$) and temperature ($T$) are strain, MPa/s and Kelvin. The empirical constants are defined as: ϖ = 37.500 MPa; $\varpi'\times$= 17.169 MPa; ϑ = −0.165; ϑ' = −0.165; ς= 0.548 s^{-1}; ς'= 0.265 s^{-1}; φ = −175.119 MPa·Kelvin and φ' =−238.562 MPa·Kelvin, with correlation coefficients (R^2) equal to 0.979 at failure and 0.970 at dilation.

8. Strain Energy Density Criterion

The strain energy density principle is applied here to describe the salt strength and deformability under different loading rates and temperatures. A similar approach has been used by Fuenkajorn et al. [6] to derive a loading rate dependent strength for salt. The distortional strain energy at failure (W_d) and at dilation ($W_{d,d}$) can be calculated from the octahedral shear stresses and strains for each salt specimen using the relations given by Jaeger et al. [10]:

$$W_d = (3/2)\cdot\tau_{oct,f}\cdot\gamma_{oct,f} \tag{7}$$

$$W_{d,d} = (3/2)\cdot\tau_{oct,d}\cdot\gamma_{oct,d} \tag{8}$$

The distortion strain energy at dilation ($W_{d,d}$) is presented as a function of the mean strain energy density at dilation ($W_{m,d}$) which can be calculated from σ_m and ε_m as follows:

$$W_{m,d} = (3/2)\cdot\sigma_{m,d}\cdot\varepsilon_{m,d} \tag{9}$$

Figure 2 shows a linear relation of $W_{d,d}-W_{m,d}$ which can be represented by:

$$W_{m,d} = 1.370W_{m,d} - 0.004 \quad \text{(MPa)} \tag{10}$$

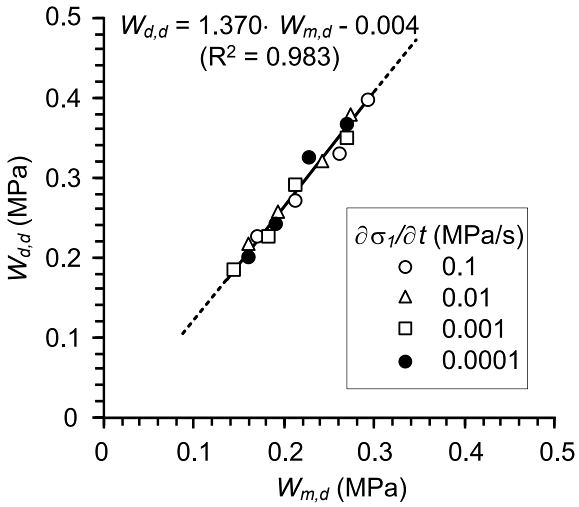

Figure 2 Distortional strain energy at dilation ($W_{d,d}$) as a function of mean strain energy at dilation ($W_{m,d}$)

The proposed criterion considers both stress and strain at dilation, and hence isolating the effect of stress rate and temperature. If the salt temperature is known, its strength can be determined from equation (10) regardless the loading rate.

9. Withdrawal Rate of Compressed-Air Energy Storage Cavern

This section describes the results of finite difference analysis using FLAC [11] for the simulations of the single isolated cavern in axial symmetry. The cavern is an up-right cylinder with the casing shoe (cavern top) at 500 m. The cavern diameter and height are 50 m and 300 m. The principal stresses and strains induced at the cavern boundary under various air withdrawal rates are calculated and compared against the dilation criteria developed above.

The in-situ stress is assumed to be hydrostatic. Before cavern development the salt stress at the casing shoe depth (σ_{cs}) is calculated as 10.8 MPa. The maximum cavern pressure is defined as 9.7 MPa (or $0.9\sigma_{cs}$). Two cases with different minimum pressures that are commonly used for the CAES caverns are studied: 1.1 MPa and 2.2 MPa ($0.1\sigma_{cs}$ and $0.2\sigma_{cs}$). Each case is simulated for four different rates of cavern pressure withdrawal: 17.3, 8.6, 0.6 and 0.3 MPa/day (equivalent to pressure schemes of 1cycle/day, 15cycles/month, 1 cycle/month and 6 cycles/year, respectively). The equivalent pressure schemes are calculated by assuming that the air injection and retrieval periods are equal. The Maha Sarakham salt is assumed to behave as a Burgers material. The Burgers constitutive equation is a built-in program in FLAC as follows:

$$\gamma_{oct} = \tau_{oct}\left[\left(\frac{t}{\eta_1}+\frac{1}{E_1}+\frac{\eta_1}{\eta_2 E_2}\right)-\left(\frac{\eta_1}{\eta_2 E_2}\exp\left(\frac{-E_2 t}{\eta_2}\right)\right)\right] \tag{11}$$

where τ_{oct} is octahedral shear stresses (MPa), t is time (day), E_1 is elastic modulus (GPa), E_2 is spring constant in visco-elastic phase (GPa), η_1 is visco-plastic coefficient in steady-state phase (GPa.day) and η_2 is visco-elastic coefficient in transient phase (GPa.day).

10. Factor of Safety Calculation

For a conservative design the surrounding salt is not allowed to dilate during the withdrawal period. This is to ensure the long-term stability of the storage cavern under loading. As a result the three dilation criteria developed above are used here to calculate the factor of safety (FS) of the salt at the bottom of the cavern where it subjects to the greatest shear stresses. These include $\tau_{oct,d}-\partial\tau_{oct}/\partial t$ criterion (equation 4), $\tau_{oct,d}$-$\gamma_{oct,d}$ criterion (equation 6) and $W_{d,d}-W_{m,d}$ criterion (equation 10).

The FS calculation methods and results for all pressure schemes are shown in Table 2. The three criteria give different FS values. The $\tau_{oct,d}$-$\gamma_{oct,d}$ criterion tends to give the highest FS values for all cases. This criterion does not consider the mean stresses and strains induced around the cavern. The $W_{d,d}-W_{m,d}$ criterion gives the most conservative results. It shows the FS values lower than 1.0 for the withdrawal rates of 15.0 and 7.5 MPa/day (1 cycle/day and 15 cycles/month). This criterion is perhaps the most appropriate for use in the design of the withdrawal rate because it incorporates both shear and mean stresses and strains. The FS values obtained from applying the $\tau_{oct,d}-\partial\tau_{oct}/\partial t$ criterion are between those obtained from the other two criteria. This criterion does not consider the mean stresses and strains induced around the cavern. The simulation results indicate that the safe maximum withdrawal rate can be increased by raising the minimum storage pressure. As shown in Tables 2, for all criteria the factors of safety calculated for the 20% minimum pressure is about 1-5% greater than those for the 10% minimum pressure.

11. Discussions and Conclusions

The salt strengths increase with loading rates which agree with the results obtained elsewhere [5-6]. The decreases of the compressive strengths with increasing temperatures also agree with the experimental results obtained by Sriapai et al. [7] and Vosteen and Schellschmidt [8]. The decrease of the salt strength as the temperature increases suggests that the applied thermal energy before the mechanical testing makes the salt weaker, and more plastic, failing at lower stress and higher strain with lower elastic moduli. The exponential creep law well represents the salt creep under compression and isothermal condition. It can describe the creep strain for all tested temperatures.

Three forms of the dilation criteria have been proposed. The $W_{d,d}-W_{m,d}$ criterion (equation 10) is the most comprehensive formulation, and perhaps is the most reliable. The $\tau_{oct,d}-\partial\tau_{oct}/\partial t$ criterion (equation 4) is the simplest. They do not consider the induced strains, but explicitly incorporate the effects of the shear rate and temperature into their formulation. The shear strains induced at dilation is added into the formulation of the $\tau_{oct,d}$-$\gamma_{oct,d}$ criterion (equation 6) to

Table 2 Factor of safety at cavern bottom based on criteria

	Factor of safety					
	$\tau_{oct,d}-\partial\tau_{oct}/\partial t$ criterion		$\tau_{oct,d}$-$\gamma_{oct,d}$ criterion		$W_{d,d}-W_{m,d}$ criterion	
Pressure scheme \ Minimum pressure (MPa)	2.2	1.1	2.2	1.1	2.2	1.1
1 cycle/day	0.78	0.74	0.38	0.36	0.33	0.36
15cycles/month	0.77	0.75	0.66	0.65	0.53	0.51
1 cycle/month	1.11	1.06	1.03	1.08	1.15	1.01
6 cycles/year	1.22	1.07	1.30	1.14	1.28	1.14

implicitly consider the rate and temperature effects. The stresses and strains of the surrounding salt needed in the safety factor calculation may be obtained from a numerical analysis. The proposed criteria may be used in the design of the suitable withdrawal rate, cavern geometry, spacing and storage scheme. The Burgers model has been used in the FLAC simulation because it is one of the simple models that can describe the instantaneous response, transient and steady-state creep of the salt. Based on this study, the CAES cavern at 500 m depth should be operated under 1 cycle/month up to 6 cycles/year. The strain energy criterion that considers both distortional and mean stress-strains at dilation tends to give the most conservative results as compared to the conventional design where the effects of loading rate have never been considered.

Acknowledgements

This study is funded by Suranaree University of Technology and by the Higher Education Promotion and National Research University of Thailand. Permission to publish this paper is gratefully acknowledged.

References

[1] Hunsche, U. & Hampel, A. (1999). Rock salt - the mechanical properties of the host rock material for a radioactive waste repository. Engineering Geology 52, 271-291.

[2] Jin, J. & Cristescu, N. D. (1998). An elastic/viscoplastic model for transient creep of rock salt. International Journal of Plasticity 14, No. 1-3, 85-107.

[3] Yang, C., Daemen, J. J. K. & Yin, J. H. (1999). Experimental investigation of creep behavior of salt rock. International Journal of Rock Mechanics and Mining Science 36, 233-242.

[4] Aubertin, M., Julien, M. R., Servant, S. & Gill, D. E. (1999). A rate-dependent model for the ductile behavior of salt rocks. Canadian Geotechnical Journal 36, 660-674.

[5] Dubey, R. K. & Gairola, V. K. (2005). Influence of stress rate on rheology-An experimental study on rocksalt of Simla Himalaya, India. Geotechnical and Geological Engineering 23, 757-772.

[6] Fuenkajorn, K., Sriapai, T. & Samsri, P. (2012). Effects of loading rate on strength and deformability of Maha Sarakham salt. Engineering Geology 135-136, 10-23.

[7] Sriapai, T., Walsri, C. & Fuenkajorn, K. (2012). Effect of temperature on compressive and tensile strengths of salt. Science Asia 38, 166-174.

[8] Vosteen, H. D. & Schellschmidt, R. (2003). Influence of temperature on thermal conductivity, thermal capacity and thermal diffusivity for different types of rock. *Physics and Chemistry of the Earth* 28, 499-509.

[9] Tabakh, M. E., Utha-Aroon, C. & Schreiber, B. C. (1999). Sedimentology of the Cretaceous Maha Sarakham evaporites in the Khorat Plateau of northeastern Thailand. *Sedimentary Geology* **123**, 31-62.

[10] Jaeger, J. C., Cook, N. G. W. & Zimmerman, R. W. (ed.) Fundamentals of Rock Mechanics, 4th edn. Chapman and Hall, London, 2007.

[11] Itasca. (1992) .User Manual for FLAC-Fast Langrangian Analysis of Continua, Version 4.0, Itasca Consulting Group Inc., Minneapolis, Minnesota.